

Photoelectrochemical Voltage vs Back Contact Barrier Heights



WPI

A Major Qualifying Project Report
Submitted to the Faculty of
WORCESTER POLYTECHNIC INSTITUTE
in partial fulfillment of the requirements for the
Degree of Bachelor of Science in Chemistry
By:

Margaret Ann Russell

Approved:

Professor Ronald L. Grimm, Primary Advisor
Department of Chemistry and Biochemistry

This report represents the work of WPI undergraduate students submitted to the faculty as evidence of completion of a degree requirement. WPI routinely publishes these reports on its website without editorial or peer review. For more information about the projects program at WPI, please see <http://www.wpi.edu/academics/ugradstudies/project-learning.html>

Table of Contents

| | |
|-------------------------------------------------------------|----|
| Table of Contents | 2 |
| Table of Figures | 3 |
| Abstract..... | 4 |
| Introduction | 5 |
| An Introduction to Solar Power | 5 |
| Semiconductor-Liquid Junctions | 7 |
| Open Circuit Voltage | 8 |
| Project Goal..... | 9 |
| Experimental..... | 10 |
| Hypothesis Calculations | 10 |
| Preparation of N-Si (111) | 11 |
| Chemicals Employed Photoelectrochemical Experiments | 11 |
| Thin-Layer Photoelectrochemistry | 13 |
| Differential Capacitance Potential | 14 |
| Results..... | 15 |
| Differential Capacitance Potential | 15 |
| Voc as a Function of the Back Contact..... | 16 |
| Discussion..... | 19 |
| Future Works..... | 20 |
| References | 22 |
| Appendix One: Photoelectrochemistry | 24 |
| Appendix Two: Impedance | 28 |
| Appendix Three: Ag/Ag ⁺ Reference Electrode..... | 31 |

Table of Figures

| | |
|---------------------------------------------------|----|
| Figure One: Traditional Solar Cell | 7 |
| Figure Two: Photoelectrochemical Cell..... | 14 |
| Figure Three: Differential Capacitance Data | 15 |
| Figure Four: Open Circuit Voltage Plot..... | 17 |
| Table One: Open Circuit Voltage Data..... | 18 |
| Figure Six: Open Circuit Voltage Graph | 19 |

1. Abstract

Many of the properties relevant to solar energy conversion in a liquid-semiconductor-liquid cell are not understood, particularly at the back, “Ohmic” contact to the semiconductor. The goal of this project is to study how the back contact affects the cell voltage. We hypothesized that the open-circuit voltage of a dual-liquid-junction photoelectrochemical cell under illumination would decrease in a 1:1 relationship with an increase in the barrier height potential at the back contact. We employed a thin layer cell with H-terminated n-type silicon as the semiconductor was used along with non-aqueous metallocene-based redox couples that demonstrate facile, 1-electron transfer. We observed decreasing open-circuit voltage values as potential energy of the redox couples shifted to more positive potentials, which correspond to increasing barrier heights for n-Si electrodes. Voltage values do not follow the perfect 1:1 relationship as predicted by the model but the relationship between open-circuit voltage and back-contact redox potential energy supports the hypothesis. We discuss how the results enable more detailed analyses of surface chemistry and what factors influence energy conversion. We further include data acquisition methodology including electrochemical impedance spectroscopy techniques and a near-term outlook for ongoing MQP projects in the Grimmgroup.

2. Introduction

2.1. An Introduction to Solar Power

In recent years, renewable energy has become increasingly popular due to growing concerns about global warming. Renewable energy comes from natural renewable sources and in 2009 they accounted for 8% of all energy used in the US and 18% of all energy used globally.¹⁻² Solar energy has been growing in popularity, from 2008 to 2015 the amount of solar power installed increased more than 23 times. One reason for the increased interest is that solar is the most abundant energy resource on earth, 173,000 terawatts of solar power strikes the earth contiguously each day, which is more than 10,000 times the world's total rate of energy use.³ Solar cells, often called photovoltaic cells, are often made up of semiconductors. Inside of the semiconductor there are various stages that make up the cell. The conduction band is the lowest vacant electronic state and the valence band is the highest possible level of electron energy. Between the two is the Fermi level that is the total electrochemical potential for the electrons. When the sun shines on the solar cell electrons are excited causing the semiconductor to produce energy. The band gap is the energy difference between the top of the valence band and the bottom of the conduction band. Recombination occurs when an electron loses energy and returns to the conduction band to stabilize itself, combining with a hole in the process. The absorption of light $h\nu > E_g$ results in the promotion of an electron from the valence band to the conduction band. Net electric current results from the journey that electron takes back to the valence band that does not involve recombination.⁴

When a contact is made with a semiconductor and a liquid, electrons lower their energy by moving from the liquid to the conduction band in the semiconductor.⁵ This causes the bands in the semiconductor to deform so the fermi levels are the same and the fermi level becomes 'pinned' in a specific location.⁶ This movement in the Fermi level is called band bending. The energy difference between the conduction band and

the fermi level is called the barrier height.⁷ Photoelectrochemical cells can be used to test these properties to understand how they affect the V_{oc} .

There are two different types of contacts that can be formed between the metal (or liquid) and the semiconductor. First is an Ohmic contact that creates a linear relationship between the current and the voltage and the contacts do not limit the current.⁸ Alternatively, a rectifying contact occurs when the electrons can only move in one direction and must overcome a bias based on the charge applied such that the electrons must overcome a barrier.⁹ An ideal semiconductor should show a linear trend when the V_{oc} values are compared to the effective solution potential.¹⁰ These contacts effect how the electrons move through the cell.

There are many contacts a semiconductor can make in order to bend the bands and collect current. When a p-type semiconductor comes into contact with an n-type of the same semiconductor and the bands bend it is called a homojunction solar cell. In a heterojunction solar cell, two different semiconducting materials compromise the n-type and p-type materials. In a Schottky-style solar cell, a metal is used to form the contacting phase with either a p-type or n-type semiconductor. Finally, a semiconductor-liquid junction behaves similarly to a Schottkey contact, but instead of metal the contact phase is a redox couple that can move charge carriers to and from the surface.

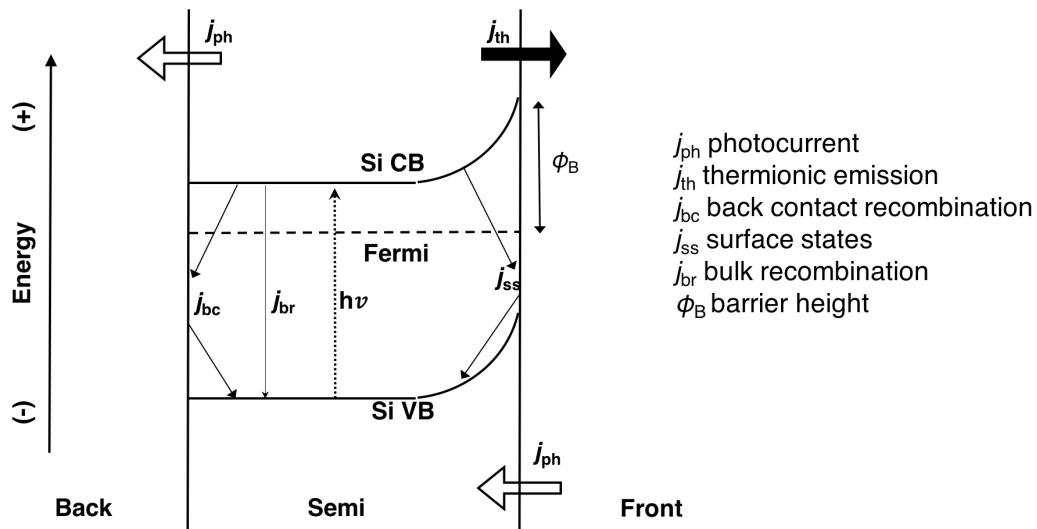


Figure 1. Traditional Solar Cell. The figure above depicts an n-type silicon solar cell with band bending at the front contact.

2.2. Semiconductor-Liquid Junctions

In photoelectrochemistry a semiconductor-liquid junction is employed, where against the front and back contact of the semiconductor a liquid is placed that can manipulate the band edge potentials so it can produce a specific voltage. This would be especially desirable in water splitting where the band edge potentials have to be positioned favorably in respect to the half reactions for O_2 evolution and H_2 evolution for solar fuel to be produced.¹¹ The ability to increase the voltage would also be helpful in creating efficient solar cells that could produce more energy.

There are various different semiconductors that can be used to solar cell. An extrinsic semiconductor has been doped to give it different electrical properties. There are two classifications of extrinsic semiconductors, p-type and n-type. P-type semiconductors have a larger concentration of hole than electrons compared to n-type semiconductors which have a larger concentration of electrons than holes.¹² In a semiconductor-liquid junction, n-type will be used in this example, the work function of the metal is smaller than the work function of the semiconductor. The work function is

the fermi energy of the metal. Understanding how semiconductor types function can help explain why *specific* V_{oc} values occur.

2.3. Open Circuit Voltage

The open circuit voltage, often called V_{oc} , reflects a change in the quasi-Fermi levels is a measure of the amount of voltage moving through the cell. Definitions of V_{oc} vary based on derivations of the majority vs the minority carrier current, and various simplifications.¹³⁻¹⁴ Solar cell V_{oc} is a kinetic balance between photocurrent (j_{ph}) and the other ‘dark’ currents in the cell. Dark current is the residual current that flows through a cell when there is no illumination, and consists of j_{th} , j_{bc} , j_{ss} , and j_{br} . Equation 1 specifies the net current, j , as a function of bias voltage, V , and photocurrent, j_{ph} , when dominated by thermionic emission in the absence of other dark current processes, i.e. $j_{bc} = j_{ss} = j_{br} = 0$.

$$j = AT^2 \exp\left(\frac{-q\phi_{B,f}}{kT}\right) \left(\exp\left(\frac{qV_{oc}}{kT}\right) - 1\right) - j_{ph} \cong AT^2 \exp\left(\frac{-q\phi_{B,f}}{kT}\right) \exp\left(\frac{qV_{oc}}{kT}\right) - j_{ph} \quad (1)$$

At no net current, $j=0$, the voltage under illumination is termed the open-circuit voltage, $V(j=0) \equiv V_{oc}$, and is given by eq 2.

$$V_{oc} = \phi_{B,f} + \frac{kT}{q} \ln \frac{j_{ph}}{AT^2} \quad (2)$$

In eqs 1 and 2, A is the Richardson constant, which is $112 \text{ A cm}^{-2} \text{ K}^{-2}$ for n-Si; q is the fundamental unit of charge, or $1.602 \times 10^{-19} \text{ C}$; k is the Boltzmann constant, $1.38 \times 10^{-23} \text{ J K}^{-1}$; T is temperature, 298 K ; and $\phi_{B,f}$ is the barrier height for the front contact, which can take any value between 0 V and $q^{-1}E_g$ (1.12 V for silicon).¹⁵ The term $\frac{kT}{q} \ln \frac{j_{ph}}{AT^2}$ will always be negative because j_{ph} is much smaller than AT^2 . Using this equation, the maximum V_{oc} for silicon can be found as exhibited in eq 3 where j_{ph} is 25 mA cm^{-2} , which is a typical photocurrent density for polished silicon under 1 “Sun” of light.

$$V_{oc} = 1.12 \text{ V} + \frac{1.38 \times 10^{-23} \frac{\text{J}}{\text{K}} 298 \text{ K}}{1.602 \times 10^{-19} \text{ C}} \ln \frac{25 \frac{\text{mA}}{\text{cm}^2}}{112000 \frac{\text{mA}}{\text{cm}^2 \text{K}^2} 298 \text{ K}^2} \quad (3)$$

Under the assumptions of ideal behavior and dark current dominated by j_{th} and no other dark processes, the highest V_{oc} n-type Si can achieve is 0.611 V. Using these eqs 1–3, the V_{oc} can be found for a cell where only the bands by the front contact are bent.

There have been a number of studies trying to understand the affect the front contact has on the V_{oc} . Many of these studies have included research into chemically altering the surface of the semiconductor and studying its effect on band bending and photovoltage behavior.¹⁶ Studies have also utilized different semiconductor surfaces such as TiO₂ and ZnO to study transfer properties.¹⁷⁻¹⁸ However, few studies have looked into the back liquid-semiconductor contact. The back contact is generally considered ohmic and is not included in the testing or V_{oc} computations.¹⁹ Such studies motivate the present investigation.

2.4. Project Goal

Herein, we report the photoelectrochemical behavior of n-Si electrodes upon variation of the potential of its back contact. We theorized the back contact is not necessarily Ohmic and we studied how that affects the V_{oc} . We hypothesized that a back-contact barrier height ($\phi_{B,b}$) would negatively impact the V_{oc} as seen in eq 4.

$$V_{oc} = \phi_{B,f} - \phi_{B,b} + \frac{kT}{q} \ln \frac{j_{ph}}{AT^2} \quad (4)$$

This indicates the voltage would decrease linearly with a one to one ratio as the back contact barrier height increased. We examined this by testing the voltage produced by the solar cell when the front contact is kept the same but the back contact is varied.

Instead of employing the traditional electrochemical cell that utilizes a metal back contact of fixed work function, the present experiments utilize a dual-liquid-junction thin-layer cell. The dual-liquid-junction thin-layer cell allows for redox couples to be tested at the back contact while the front contact can stay the same. The thin-layer cell allows for efficient testing of the back contact and allows for the opportunity to study

the surface chemistry of the semiconductor. We employed hydrogen-terminated n-Si(111) due to its well-understood chemical and structural properties, and in order to remove any variables such as interfacial dipoles that could affect the V_{oc} . A number of different redox couples were employed to study the effect of varying the back contact redox couple. These redox couples included ferrocene⁺⁰, cobaltocene⁺⁰, dimethylferrocene⁺⁰, octamethylferrocene⁺⁰, and decamethylferrocene⁺⁰. Ferrocene was used as the front contact facing illumination to maintain consistency in the experiments. Varying the back contact allows us to learn more about the relationship between the back contact and the V_{oc} . The experiments and simulations describe a comprehensive depiction of the chemistry and carrier dynamics of semiconductor-liquid junctions.

3. Experimental Section

3.1. Hypothesis Calculations

To arrive at eq 4 for our hypothesized relationship between V_{oc} and the back-contact barrier height, we started with eq 1 that only takes in to account $\phi_{B,f}$, and considered the photocurrent at open circuit ($j = 0$) as shown in eq 5.

$$j_{ph} = AT^2 \exp\left(\frac{-q\phi_{B,f}}{kT}\right) \exp\left(\frac{qV_{oc}}{kT}\right) \quad (5)$$

From eq 5, we assume that a barrier height at the back contact, $\phi_{B,b}$, would attenuate the photocurrent, thus reducing j_{ph} to $j_{ph} \exp\left(\frac{-q\phi_{B,b}}{kT}\right)$. Adjusting eq 5 with the attenuated photocurrent yields eq 6, with subsequent rearrangements in eqs 7–8.

$$j_{ph} \exp\left(\frac{-q\phi_{B,b}}{kT}\right) = AT^2 \exp\left(\frac{-q\phi_{B,f}}{kT}\right) \exp\left(\frac{qV_{oc}}{kT}\right) \quad (6)$$

$$\frac{j_{ph}}{AT^2} = \exp\left(\frac{-q\phi_{B,f}}{kT}\right) \exp\left(\frac{q\phi_{B,b}}{kT}\right) \exp\left(\frac{qV_{oc}}{kT}\right) \quad (7)$$

$$\ln\left(\frac{j_{ph}}{AT^2}\right) = \frac{-q\phi_{B,f}}{kT} + \frac{q\phi_{B,b}}{kT} + \frac{qV_{oc}}{kT}. \quad (8)$$

From there $\frac{q}{kT}$ was divided out and V_{oc} was solved which produced the final eq 9, which is identical to eq 4. The back-contact barrier height term is in bold to highlight the difference as compared to eq 2.

$$V_{oc} = \phi_{B,f} - \boldsymbol{\phi_{B,b}} + \frac{kT}{q} \ln \frac{j_{ph}}{AT^2} \quad (9)$$

Several important implications exist for the additional $\phi_{B,b}$ term in eq 9 as compared to eq 2. When the back contact is Ohmic, $\phi_{B,b} = 0$, and eq 9 reduces to eq 2 as expected. However, the presence of a barrier height at the back serves to directly and linearly decrease V_{oc} values concomitant with changes in $\phi_{B,b}$. Testing this relationship between $\phi_{B,b}$ and V_{oc} motivates this work.

3.2. Preparation of N-Si(111)

Phosphorus doped, n-Si(111) (Silicon Inc., Boise, Idaho, 1.3–2.5 Ω cm resistivity, 500 ± 25 μm thick, double-side polished) wafers, were diced into $\sim 2 \times 1$ cm rectangles. Diced silicon pieces were initially sonicated in isopropyl alcohol (99.9%, Fisher Scientific) for 10 minutes then rinsed with H_2O (18 $\text{M}\Omega$ cm Millipore). Following sonication, the RCA Standard Clean–1 (SC–1 or RCA–1) and Standard Clean–2 (SC–2 or RCA–2) procedures further cleaned the silicon surfaces with each reaction consisting of a ten-minute immersion. The wafers were then dried and treated with 6M $\text{HF}_{(aq)}$ (diluted from stock solution, 49%, Transene, Danvers, Massachusetts) for 10 seconds, then thoroughly rinsed in H_2O to remove any remaining chemical oxide. The samples were dried and transferred to a nitrogen-purged glove box (LABstar Glove Box Workstation, M. Braun Incorporated, Stratham, New Hampshire) for storage until needed.

3.3. Chemicals Employed in Photoelectrochemical Experiments

The mixtures employed for the experiments used nonaqueous metallocene-based redox couples along with the accompanying electrolyte. The electrochemical studies

employed five redox couples: ferrocene/ferrocenium (Cp_2Fe , ferrocene⁺⁰), cobaltocene/cobaltocenium (Cp_2Co , cobaltocene⁺⁰), decamethylferrocene/decamethylferrocenium (Cp_2^*Fe , decamethylferrocene⁺⁰), octamethylferrocene/octamethylferrocenium ($\text{Me}_8\text{Cp}_2\text{Fe}$, octamethylferrocene⁺⁰), and dimethylferrocene/dimethylferrocenium ($\text{Me}_2\text{Cp}_2\text{Fe}$, dimethylferrocene⁺⁰). Sublimation under vacuum purified the metallocenes: cobaltocene (Cp_2Co , bis(cyclopentadienyl)cobalt(II), 99%, Sigma-Aldrich), ferrocene (Cp_2Fe , bis(cyclopentadienyl)iron(II), 99%, Sigma-Aldrich), and decamethylferrocene ($\text{Me}_{10}\text{Cp}_2\text{Fe}$ or Cp_2^*Fe , bis(pentamethylcyclopentadienyl)iron(II), 99%, Sigma-Aldrich). Chemical oxidation of decamethylferrocene with *p*-quinone (98+%, Alfa Aesar) and HBF_4 (50 wt % aqueous solution, Alfa Aesar) produced decamethylferrocenium tetrafluoroborate following literature techniques. The metallocenium compounds: cobaltocenium hexafluorophosphate (Cp_2CoPF_6 , bis(pentamethylcyclopentadienyl)cobalt(III)hexafluorophosphate, 97%, Sigma-Aldrich), ferrocenium hexafluorophosphate (Cp_2FePF_6 , bis(pentamethylcyclopentadienyl)iron(III)hexafluorophosphate, 97%, Aldrich), and decamethylferrocenium tetrafluoroborate ($\text{Me}_{10}\text{Cp}_2\text{FeBF}_4$ or $\text{Cp}_2^*\text{FeBF}_4$, bis(pentamethylcyclopentadienyl) were purified through recrystallization and then degassed under a vacuum.

Octamethylferrocene ($\text{Me}_8\text{Cp}_2\text{Fe}$) was synthesized by refluxing 2.8 g of Iron (II) Chloride (FeCl_2 , anhydrous, 99.5%, Fisher Scientific) and 50 mL of Tetrahydrofuran ($\text{C}_4\text{H}_8\text{O}$, spectrophotometric grade 99.7+%, Alfa Aesar) then adding 3.0 g of Lithium Tetramethylcyclopentadiene ($\text{LiC}_5\text{H}(\text{CH}_3)_4$, 97%+, Alfa Aesar) by cannula transfer.²⁰ The solution was subsequently refluxed for 24 hours, the solvent was removed at 25 °C, and the resulting precipitate was sublimated under vacuum for several hours at 100 °C to yield long, yellow-orange needles. The octamethylferrocenium salt was prepared

utilizing the same procedure that produced dimethylferrocenium tetrafluoroborate. An Ag/Ag⁺ electrode was used to assess the purity and it affirmed the appropriate compound had been synthesized.

Lithium perchlorate (battery grade, Sigma-Aldrich) was used as received. A commercial solvent drying system (JC Meyer Solvent System, Laguna Beach, CA) supplied “dry” trichloroethylene (99.9%, Fisher Scientific) that was stored in the glove box over activated molecular sieves (3Å, 1–2 mm beads, Alfa Aesar). Propylene carbonate (99.5% anhydrous, Acros Organics) was stored over activated 3 Å molecular sieves in the glove box.

3.4. Thin-Layer Photoelectrochemistry

The methods used in the thin-layer cell followed literature techniques and can be seen in Fig. 2.²¹ A copper wire was connected to the side of an indium tin oxide (ITO) slide using GaIn liquid alloy. Inside of the glove box the front ITO glass was placed into a custom-fabricated Delrin holder (McMaster Carr, not shown in Fig. 1) facing illumination. A pipette (0.2–2 µL Fisherbrand, NU00446) was used to place 0.5–1.0 µL of the redox couple onto the slide. A silicon wafer was carefully layered on top of the first redox couple. The pipet added 0.5–1.0 µL of the redox couple to the back of the silicon wafer. A second ITO glass was layered on top of the redox couple but slightly off center due to the wire connected to the first ITO glass. Two type-304 stainless steel clamps were placed on the top of the cell to maintain uniform compression between the two ITO slides. The back ITO slide that faces away from illumination connected to the working electrode and the front ITO slide that faces the illumination connected to the reference and counter electrode connections. The potentiostat (Biologic, SP-300) measured and recorded the desired values.

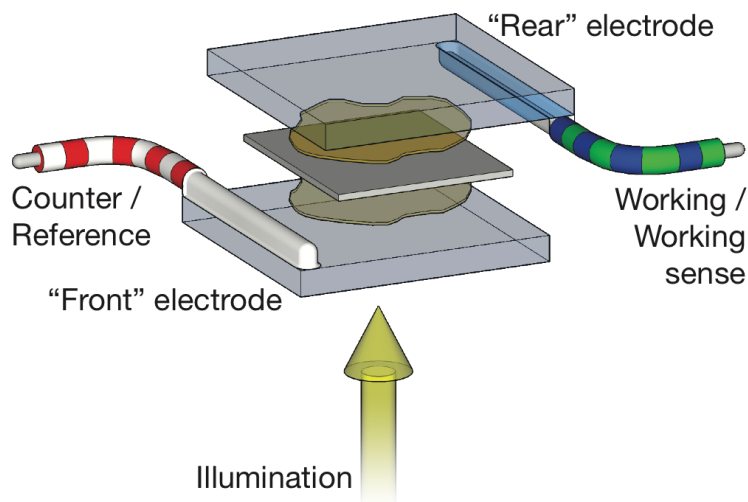


Figure 2. Experimental setup employed for the dual thin-layer photoelectrochemistry cell.

3.5. Differential Capacitance Potential

Two different setups were used to perform the differential capacitance potential experiments. The thin layer cell was used and setup as previously mentioned for the tests involving both ferrocene and cobaltocene. Ferrocene was used as the front contact and cobaltocene was used as the back. For the gallium indium experiments the thin layer cell was used. 0.5–1.0 μL of ferrocene was placed onto an ITO glass and on top of that was placed a piece of gallium indium that was connected to a wire. The appropriate tests were taken. The data was fit using a program called LabVIEW. The data was loaded in and fit so outlier data was not included. Each point was fit by itself and the overall data could not be viewed during that fitting. This was done so the final graph and overall data was not considered or used to obstruct the fit of the individual points. Eq 10 was used to determine the flat-band potential.

$$E_{\text{fb}} = E(C^{-2} = 0) - \frac{kT}{q} \quad (10)$$

Eq 11 determined the barrier height in n-type Si based on the extrapolated flat-band potential.

$$\phi_{B,n} = E_{fb} + \frac{kT}{q} \ln \frac{N_D}{N_C} \quad (11)$$

N_D is the dopant density of the semiconductor, which is $1 \times 10^{15} \frac{1}{cm^3}$ for n-type Si, and N_C is the density of states in the conduction, which is $3.2 \times 10^{19} \frac{1}{cm^3}$.²²

4. Results

4.1. Differential Capacitance Potential

Figure three presents the area-corrected differential capacitance–potential ($A^2C_{diff}^{-2}$ vs E) of a thin layer cell using hydrogen-terminated n-Si (111) plotted with the electrode area corrected for differential capacitance as the y-axis and potential as the x-axis. Cp_2Fe was used as the front contact facing illumination and Cp_2Co as the back contact farther away from illumination.

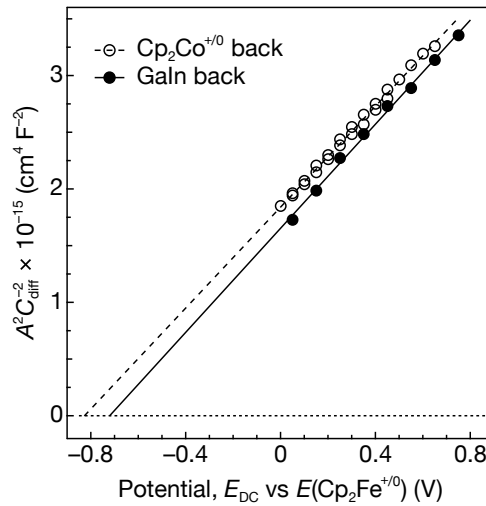


Figure 3. Differential capacitance potential measured in the thin layer cell with ferrocene (Cp_2Fe) as the front contact and cobaltocene (Cp_2Co) as the back contact with hydrogen-terminated n-Si (111).

By plugging the potential, roughly $-0.83V$, found in this experiment into eq 10 the flat band potential was determined to be $-0.26V$.

$$E_{fb} = -0.83V - 25V$$

That number was then placed into eq 11 to determine the barrier height for n-type silicon.

$$\phi_{bn} = \frac{-0.26V}{1C} - 0.25V \ln\left(\frac{1 \times 10^{15} \frac{1}{\text{cm}^3}}{3.2 \times 10^{19} \frac{1}{\text{cm}^3}}\right)$$

The back contact barrier height is -0.46V.

4.2. V_{oc} as a Function of the Back-Contact Potential

Figure 4 demonstrates photocurrent density potential (J-E) traces for the thin layer cell using hydrogen-terminated n-Si (111) where Cp_2Fe is used as the front contact. Measurements were taken under ELI-simulated 100 mW cm^{-2} illumination. The solid line corresponds to measurements taken with Cp_2Co as the back contact and represents the $V_{oc} = -450 \pm 20 \text{ mV}$. the dashed line corresponds to measurements taken with $\text{Me}_2\text{Cp}_2\text{Fe}$ as the back contact and represents the $V_{oc} = -170 \pm 90 \text{ mV}$. This cell has a highly resistive current density which does not reach the light limited plateau and a fill factor of 0.25. This is attributed to the resistive behavior from insufficient compression that leads to the liquid being too thick inside of the cell to achieve the thickness needed to match the diffusion length of the metallocene species and the lithium perchlorate in the propylene carbonate.

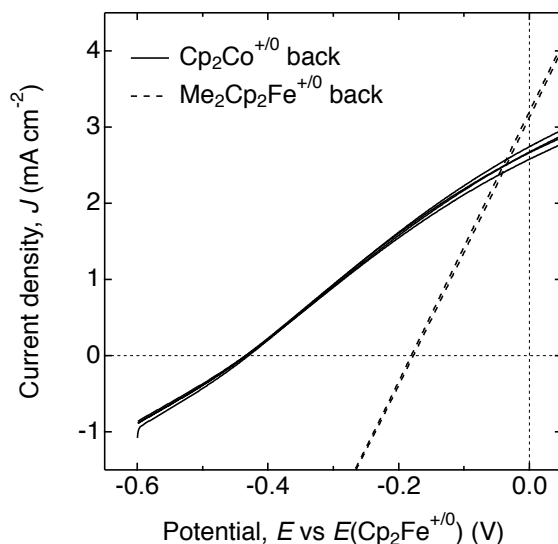


Figure 4. Open circuit voltage plot. Photocurrent density potential (J-E) measured in the thin layer cell with ferrocene (Cp_2Fe) as the front contact and cobaltocene (Cp_2Co) as the back contact with hydrogen-terminated n-Si (111). The solid lines correspond to scans taken under ELH-simulated 100mW cm^{-2} illumination while the dashed lines correspond to scans taken in the dark.

Table 1 presents the open-circuit photovoltage, V_{oc} , results for the hydrogen terminated n-Si (111) in a dual thin-layer photoelectrochemical cell as a function of the back contact. All measurements were taken with ELH-simulated 100 mW cm^{-2} illumination using ferrocene ($\text{Cp}_2\text{Fe}^{+/0}$) as the front contact. The table contains the sample number, back contact, V_{oc} , margin of error, number of trials and the half wave potentials. The half wave potential demonstrates the formal potential for the redox couple vs. the ferrocene formal potential.

| Case Number | Back Redox Couple | V_{oc} (V) | Num. Samples | E^o vs $E(\text{Fc}^{+/0})$ (V) |
|-------------|-----------------------------------------------|--------------------|--------------|-----------------------------------|
| 1 | $\text{Cp}_2\text{Co}^{+/0}$ | -0.446 ± 0.023 | 4 | -1.33 |
| 2 | $(\text{CpCO}_2\text{CH}_3)_2\text{Co}^{+/0}$ | ~ -0.4 (est) | | -0.763 |
| 3 | $\text{Cp}^*_2\text{Fe}^{+/0}$ | -0.310 ± 0.010 | 4 | -0.468 |
| 4 | $\text{Me}_8\text{Cp}_2\text{Fe}^{+/0}$ | -0.290 ± 0.030 | 4 | -0.406 |
| 5 | $\text{Me}_2\text{Cp}_2\text{Fe}^{+/0}$ | -0.170 ± 0.009 | 3 | -0.1 |
| 6 | $\text{Cp}_2\text{Fe}^{+/0}$ | -0.050 ± 0.020 | 4 | 0 |
| 7 | $\text{Cp}(\text{COCH}_3)\text{CpFe}^{+/0}$ | $\sim +0.1$ (est) | | 0.261 |

Table 1. Open-circuit voltage data. Open-circuit photovoltage, V_{oc} , for n-Si(111) electrodes measured in a thin layer cell under illumination with ELH-simulated 1 sun illumination. All redox couple solutions consist of 100 mM for the species that accepted the minority photocarriers, and 50 mM for the species that accepted the majority carriers, and 1M LiClO_4 in propylene carbonate.

Figure seven plots V_{oc} versus the effective solution potential vs E (Cp_2Fe) using hydrogen terminated n-Si(111) electrodes under ELH-simulated 100 mW cm^{-2} illumination. Cp_2Fe was used as the front contact and the back contact was varied and the error bars were added to show the possible error in measurement. Moving from right to left across the x -axis and from up to down across the y -axis the points correspond to the following redox couples in descending order: $\text{Cp}(\text{COCH}_3)\text{CpFe}^{+/0}$, $\text{Cp}_2\text{Fe}^{+/0}$, $\text{Me}_8\text{Cp}_2\text{Fe}^{+/0}$, $\text{Me}_2\text{Cp}_2\text{Fe}^{+/0}$, $\text{Cp}^*_2\text{Fe}^{+/0}$, $\text{Cp}_2\text{Co}^{+/0}$, and $(\text{CpCO}_2\text{CH}_3)_2\text{Co}^{+/0}$. The line serves as a guide to indicate an overall trend in the behavior of the back contact.

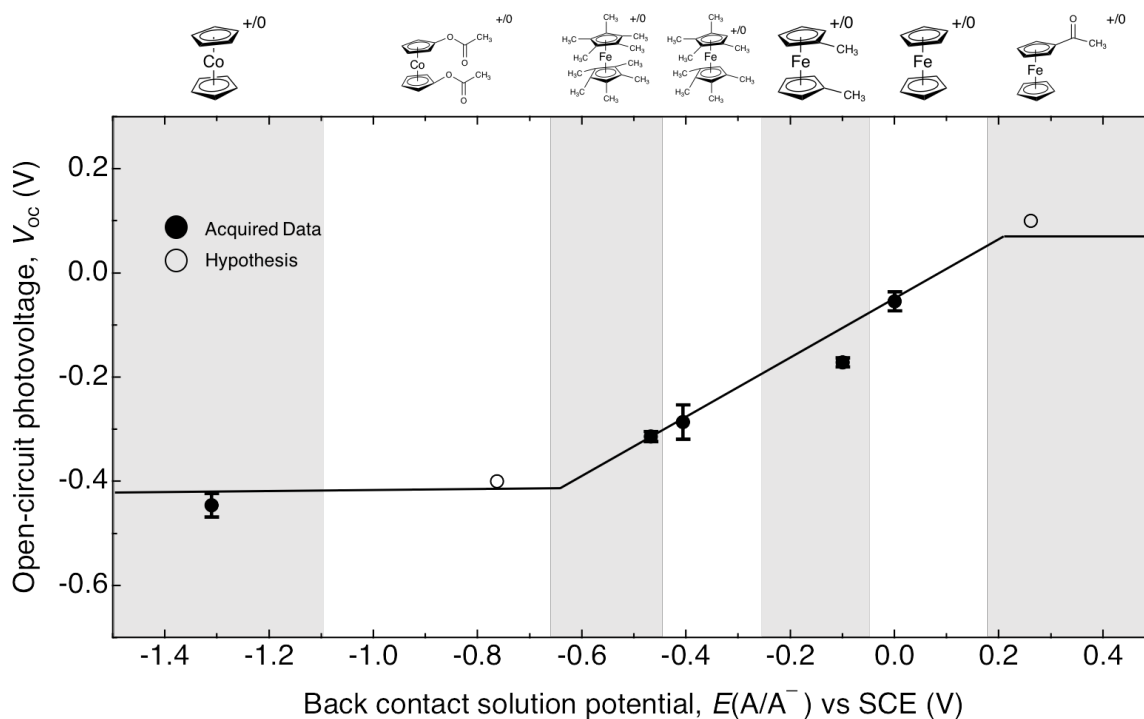


Figure 5. Open circuit voltage graph. Open circuit voltage versus the effective solution potential vs. $E(\text{Cp}_2\text{Fe})$ with ferrocene (Cp_2Fe) used as the front contact while the back contact was varied. The solid line acts as a guide to show the overall trend in the behavior.

5. Discussion

By analyzing the results of the various experiments, we were able to understand more about the relationship between the back contact and photoelectrochemical voltage. As seen in figure five when the open circuit voltage, or V_{oc} , is compared to the redox solution potential there is a one to one linear slope. The linear trend shows the junction between the two is not ohmic and the back contact does deleteriously affect V_{oc} .

The solution redox potentials position affects the V_{oc} . When the solution potential is above the conduction band edge there is no barrier, the back contact is ohmic, and large V_{oc} values are observed as is the case with Cp_2Co . When the solution potential is between the semiconductor valence band and conduction band the V_{oc} scales one to one with the solution potential. This indicates the hypothesis is correct the back contact does affect the V_{oc} so eq 9 is valid.

$$V_{oc} = \phi_{B,f} - \phi_{B,b} + \frac{kT}{q} \ln \frac{j_{ph}}{AT^2} \quad (9)$$

is valid. So to obtain a high open circuit voltage factors that lead to barriers at the back contact such as surface states and non-ideal contacts should be avoided.

The barrier height was measured and calculated from the differential capacitance potential experiment. The thermodynamic limit for V_{oc} in n-type silicon is 0.7V, since about 0.4V are lost to recombination. The absolute value of the barrier height measured in the impedance tests was 0.46V, which is close to the absolute value of the measured V_{oc} using the same front and back contact, 0.446V. This indicates there is a barrier height.

The linear slope of the V_{oc} vs. redox solution potential also indicates the back contact is ideal. In an ideal contact the metal and liquid are in contact on the atomic scale however the components do not intermix. So there are no surface charges or absorbed impurities at the interface. This means that experiments studying changes in the surface chemistry of the semiconductor can be performed and the back contact will not affect the results. Additionally, the accuracy of these results indicate that the thin layer liquid cell can produce accurate results so it can be used in future experiments.

6. Future work

Future goals for this project would be to test different semiconductors and redox couples in the thin layer cell. The thin layer cell is an efficient way to measure the open circuit voltage so it would be an effective way to test various types of semiconductors. This could include but is not limited to methylated silicon, perovskites, and various sulfides. Specifically, with the methylated silicon it would be interesting to see how it compared to the hydrogen terminated silicon when the same redox couples are used. Additionally, testing other redox couples to see how the trend continues could produce

noteworthy results. The thin layer cell is an interesting way to study photoelectrochemistry and there are a number of different directions this project could take.

7. References

¹ "Renewable Energy Quick Facts." *American Physical Society*. N.p., n.d. Web. 25 Mar. 2017.

S, Jacob. "Non Renewable Facts." *LIVESTRONG.COM*. Leaf Group, 06 July 2015. Web. 25 Mar. 2017.

³ "Top 6 Things You Didn't Know About Solar Energy." *Energy.gov*. United States of America, n.d. Web. 25 Mar. 2017.

⁴ M. Peter, Laurence. "Chapter 1 Photoelectrochemistry: From Basic Principles to Photocatalysis." *Royal Society of Chemistry*. Royal Society of Chemistry, 2016. Web. 25 Mar. 2017.

⁵ Memming, Rüdiger, and Detlef Bahnemann. "Semiconductor Surfaces and Solid-Solid Junctions." *Semiconductor Electrochemistry*. Somerset: Wiley, 2001. 22-45. Print.

⁶ Bard, Allen J., Andrew B. Bocarsly, and Fu-Ren F. Fan. "The Concept of Fermi Level Pinning at Semiconductor/Liquid Junctions. Consequences for Energy Conversion Efficiency and Selection of Useful Solution Redox Couples in Solar Devices." *Journal of the American Chemical Society* 102.11 (1980): 3671-676. Print.

⁷ Memming, Rüdiger, and Detlef Bahnemann. "Semiconductor Surfaces and Solid-Solid Junctions." *Semiconductor Electrochemistry*. Somerset: Wiley, 2001. 22-45. Print.

⁸ "Metal-Semiconductor Junction – Ohmic Contact." *DoITPoMS*. University of Cambridge, 2015. Web. 21 Mar. 2017.

⁹ "Metal-Semiconductor Junction – Rectifying Contact." *DoITPoMS*. University of Cambridge, 2015. Web. 25 Mar. 2017.

¹⁰ Grimm, Ronald L., Matthew J. Bierman, Leslie E. O'Leary, Nicholas C. Strandwitz, Bruce S. Brunschwig, and Nathan S. Lewis. "Comparison of the Photoelectrochemical Behavior of H-Terminated and Methyl-Terminated Si(111) Surfaces in Contact with a

Series of One-Electron, Outer-Sphere Redox Couples in CH₃CN." *The Journal of Physical Chemistry C* 116.44 (2012): 23569-3576. Web. <10.1021/jp308461q>.

¹¹ Landman, Avigail, Hen Dotan, and Gennady E. Shter. "Photoelectrochemical Water Splitting in Separate Oxygen and Hydrogen Cells." *Nature Materials* (n.d.): n. pag. *Nature Materials*. Nature, 13 Mar. 2017. Web. 21 Mar. 2017. <doi:10.1038/nmat4876>.

¹² "Metal-Semiconductor Junction – Rectifying Contact." *DoITPoMS*. University of Cambridge, 2015. Web. 25 Mar. 2017.

¹³ Memming, Rüdiger, and Detlef Bahnemann. "Charge Transfer Processes at the Semiconductor-Liquid Interface." *Semiconductor Electrochemistry*. Somerset: Wiley, 2001. 151-240. Print.

¹⁴ Lewis, Nathan S. "A Quantitative Investigation of the Open-Circuit Photovoltage at the Semiconductor/Liquid Interface." *Journal of the Electrochemical Society* 131.11 (n.d.): 2496-503. 24 Jan. 1984. Web. <doi: 10.1149/1.2115347>.

¹⁵ Maldonado, Stephen, Katherine E. Plass, David Knapp, and Nathan S. Lewis. "Electrical Properties of Junctions between Hg and Si(111) Surfaces Functionalized with Short-Chain Alkyls." *The Journal of Physical Chemistry C* 111.48 (2007): 17690-7699. Web. <10.1021/jp070651i>.

¹⁶ Lewis, Nathan S. "A Quantitative Investigation of the Open-Circuit Photovoltage at the Semiconductor/Liquid Interface." *Journal of the Electrochemical Society* 131.11 (n.d.): 2496-503. 24 Jan. 1984. Web. <doi: 10.1149/1.2115347>.

¹⁷ Rowley, J. G.; Ardo, S.; Sun, Y.; Castellano, F. N.; Meyer, G. J., Charge Recombination to Oxidized Iodide in Dye-Sensitized Solar Cells. *J. Phys. Chem. C* 2011, 115, 20316-20325.

¹⁸ O'Donnell, R. M.; Sampaio, R. N.; Barr, T. J.; Meyer, G. J., Electric Fields and Charge Screening in Dye Sensitized Mesoporous Nanocrystalline TiO₂ Thin Films. *J. Phys. Chem. C* 2014, 118, 16976-16986.

¹⁹ Rosenbluth, Mary L., and Nathan S. Lewis. "Kinetic Studies of Carrier Transport and Recombination at the N-silicon Methanol Interface." *Journal of the American Chemical Society* 108.16 (1986): 4689-695. Web. <10.1021/ja00276a001>.

²⁰ Kern, W., The Evolution of Silicon Wafer Cleaning Technology. *J. Electrochem. Soc.* 1990, 137, 1887-1892.

²¹ Roghi E. Kalan, Margaret A. Russell, Jessica Taylor, and Ronald L. Grimm. *Submitted to J. Electrochem. Soc.*

²² Maldonado, Stephen, Katherine E. Plass, David Knapp, and Nathan S. Lewis. "Electrical Properties of Junctions between Hg and Si(111) Surfaces Functionalized with Short-Chain Alkyls." *The Journal of Physical Chemistry C* 111.48 (2007): 17690-7699. Web. <10.1021/jp070651i>.

1. Appendix One: Photoelectrochemistry

1.1. Acquire the Appropriate Materials

Appropriate materials include: two prepared ITO glasses, the delrin holder, multiple n-type silicon wafers, the redox couple solution, the pipette and multiple tips. Materials that should already be in the glove box include: the potentiostat wires, kimwipes, gloves, and the metal plate that can be screwed into the box to hold the setup in place.

1.2. Preparation Inside the Glove Box

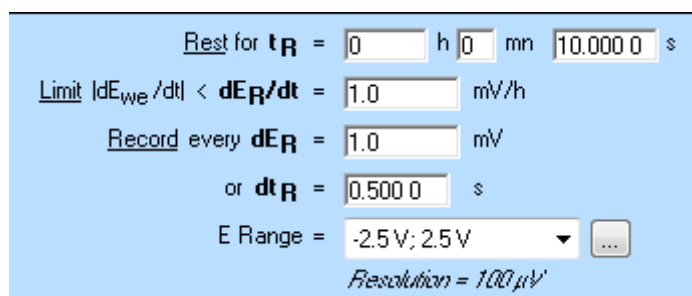
Screw the metal plate in such that the hole aligns with the hole in the bottom of the box. Screw in the delrin holder so the hole in the bottom aligns with the hole in the plate. Place the first ITO glass down so the wire side is towards the back of the holder (where it connects to the metal pole/plate).

Place the appropriate amount of the redox couple onto the center of the ITO glass. Layer the wafer on top such that it fully covers the redox couple. Place the next redox couple onto the center of the wafer. Then layer the ITO glass on top with the wire on the opposite side of the wire on the first ITO glass (towards the front opening of the hole).

Make sure not to move the cell or smear the liquid so the redox couples don't mix. Tighten the clamps on either side of the cell or place a small weighted object on top of the cell to compress it. Connect the appropriate wires from the potentiostat to the cell.

1.3. Preparation Outside the Glove Box

Turn on the potentiostat. Open up the EC-Lab program and press the connect button (it's a small plug shaped button). Next press the plus button on the column on the left hand side and say yes to switching to modify mode. Then select OCV. Load the settings listed in the picture below:



The screenshot shows the following settings in the EC-Lab software:

- Rest for t_R = 0 h 0 mn 10.000 0 s
- Limit $|dE_{we}/dt| < dE_R/dt$ = 1.0 mV/h
- Record every dE_R = 1.0 mV
- or dt_R = 0.500 0 s
- E Range = -2.5 V; 2.5 V
- Resolution = 100 μ V

Then select CV and load the settings listed in the picture below:

Set E_{we} to E_i = V vs.

Scan E_{we} with dE/dt =

to vertex potential E_1 = V vs.

Reverse scan to vertex E_2 = V vs.

Repeat n_c = time(s)

Measure <I> over the last % of the step duration

Record <I> averaged over N = voltage steps

E Range = ...

Resolution = 100 μ V

I Range = ...

Bandwidth =

End scan to E_f = V vs.

(dE/dt \sim 100 μ V / 2 ms)
 (dEN \sim 1.0 mV)
 (1400 points per cycle)

Then select CV and load the settings listed in the picture below:

Set E_{we} to E_i = V vs.

Scan E_{we} with dE/dt =

to vertex potential E_1 = V vs.

Reverse scan to vertex E_2 = V vs.

Repeat n_c = time(s)

Measure $\langle I \rangle$ over the last % of the step duration

Record $\langle I \rangle$ averaged over N = voltage steps

E Range = ...

Resolution = 100 μ V

I Range = ...

Bandwidth =

End scan to E_f = V vs.

(dE/dt ~ 100 μ V / 2 ms)
(dEN ~ 1.0 mV)
(1400 points per cycle)

So you should have one OCV and two CVs. Then click the advanced settings (in the left hand column) and check text export. Then go into the EC-Lab folder in the grimmgroup drive and create a new file for your experiment with the title: date-your initials-front contact-material type-back contact-experiment number. Turn off all the lights in the lab and shut the shades, you are now ready to start the experiment.

1.4. Experimentation

Press the green arrow on the bottom of the column on the far left, this will begin your experiment. Save your experiment to the file you created earlier. Turn the light on so it shines through the bottom of the box. Turn it on about 1 second into the first OCV. Keep it on for the OCV and the second CV and turn it off for the last CV. Repeat as needed.

1.5. Organizing the Data

Open IGOR and a new word file. Save the word file into the folder you previously used and name it the same thing as the folder. Drag the text files from the folder into IGOR then copy and paste them into the word document. Use the key combination CTRL+N to get rid of files you have already copied. Continue until you are done.

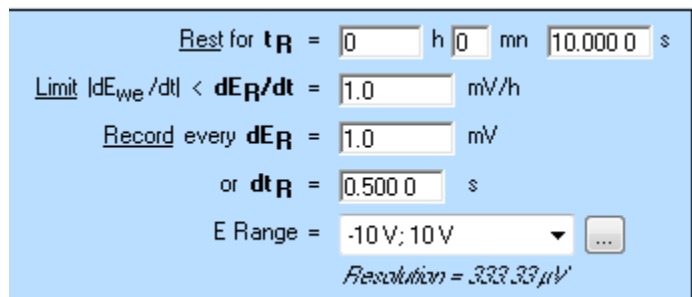
2. Appendix Two: Impedance

2.1. Preparation Inside the Glovebox

Follow the procedures from 1.1 and 1.2 of appendix one.

2.2. Preparation Outside the Glovebox

Turn on the potentiostat. Open up the EC-Lab program and press the connect button (it's a small plug shaped button). Next press the plus button on the column on the left hand side and say yes to switching to modify mode. Then select OCV. Load the settings listed in the picture below:



Then select SPEIS and load the following settings:

Mode Single Sine
 Multiple Sine

Scan E_{we} from E_i = 0.800 0 V vs. Ref
to E_f = 0.000 0 V vs. Ref
with N = 8 potential steps

For each potential step
Wait for t_s = 0 h 0 mn 5.000 s
 Record every dI = 0.000 mA
or dt = 0.100 s

Scan frequencies from f_i = 1.000 MHz
to f_f = 1.000 Hz
with N_d = 10 points per decade
or N_T = 4 points from f_i to f_f
in Logarithmic spacing
or Linear spacing Show frequencies >>

sinus amplitude V_a = 10.0 mV ($V_{rms} \sim 7.07$ mV)
wait for p_w = 0.10 period before each frequency
average N_a = 2 measure(s) per frequency
drift correction

E Range = -10 V; 10 V
Resolution = 333.33 μV
I Range = 10 mA
Bandwidth = 8

(~ 1mn03s / scan)
(dE ~ 0.100 V)

Then select SPEIS and load the following settings which allow you to scan backwards and in-between the previously collected data points:

Mode Single Sine
 Multiple Sine

Scan E_{we} from E_i = V vs.

to E_f = V vs.

with N = potential steps

For each potential step

Wait for t_s = h mn s

Record every dI = mA

or dt = s

Scan frequencies from f_i = MHz

to f_f = Hz

with N_d = points per decade

or N_T = points from f_i to f_f

in Logarithmic spacing

or Linear spacing

sinus amplitude V_a = mV ($V_{rms} \sim 7.07$ mV)

wait for p_w = period before each frequency

average N_a = measure(s) per frequency

drift correction

E Range =

Resolution = 333.33 μ V

I Range =

Bandwidth =

(~ 1mn03s / scan)
(dE ~ 0.100 V)

So you should have one OCV and two SPEISs. Then click the advanced settings (in the left hand column) and check text export. Then go into the EC-Lab folder in the grimmgroup drive and create a new file for your experiment with the title: date-your initials-front contact-material type-back contact-experiment number. Turn off all the lights in the lab and shut the shades, you are now ready to start the experiment.

2.1. Experimentation

Press the green arrow on the bottom of the column on the far left, this will begin your experiment. Save your experiment to the file you created earlier. Turn the light on so it shines through the bottom of the box. Turn it on about 1 second into the first OCV then turn it off for both of the SPEIS runs.

2.2. Organizing the Data

Open up LabVIEW. Select open existing: \\research.wpi.edu\grimmgroup\EIS... and click the white arrow once a screen with four graphs pops up. From there click new and load your first SPEIS file in. Move the window such that the bottom left graph is not visible. Now fit the data by dragging the red line so it fits with the open circles. Once you have gone through all the data points the graph on the bottom left should look like a straight line. Save this file then repeat the procedure with the second SPEIS file. Then save that and load both SPEIS files in and fit both. Finally save that file then import them to IGOR using the procedure listed in appendix one-1.5.

3. Appendix 3: Ag/Ag⁺ Reference Electrode

3.1. Materials

For this experiment you will need: AgNO₃ (liquid), vycor Frit Disks that are ~7mm diameter ~2mm long, needle, silver wire, small septum for the top of the glass tubing and 6mm glass tubing about 6" long.

3.2. Preparation

1. Figure out what gauge needle the Ag wire goes through to thread the catheter
2. Practice threading Ag wire into septum using a needle and a "dirty" wire
3. Figure out heat shrink situation for the glass and the frit
 1. Try using the teflon heat shrink (it's a pale white color)

-
4. Practice putting the septum on the 6mm glass outside of the glove box
 1. Try using a metal spatula to hold one side down while you push down the other side

3.3. *Cleaning*

1. Clean the Ag wire by abrading it (rubbing lightly with soft sand paper), then dip it into 10% Nitric Acid solution for 30 seconds, then rinse it off with 18-Ohmic H₂O, and dry it
 1. 1.2ml nitric acid and rest h₂O in 10 ml graduated cylinder dip for 10 min dip in aqua regia
2. Clean the glass using the standard technique (RCA 1 & 2) and then dry it in the oven overnight
3. Wipe down the metal spatula with isopropanol

3.4. *Parts to Build Outside of the Glove Box*

1. Attach the septum to the bottom of the glass tubing with heat shrink and use a heat gun (Not the soldering iron!) to shrink the heat shrink
2. Put the glass/vicor/heat shrink into the oven for a couple hours/overnight
3. Thread Ag wire into the septum using the needle with the longer end “under” (the lower bottom side) the septum
 1. Only touch the top of the Ag wire (not the end going into the filling solution)
 2. Make sure it is dry then put it directly into the glove box

3.5. *Inside the Glove Box*

1. Prepare the solvent and supporting electrolyte solution, make sure it is stirred well and fully mixed. **Do NOT add the redox species!**

-
2. Dip the glass/vicor in solvent/electrolyte solution to wet the vicor fit
 3. Add 2-3 grains of AgNO_3 to the electrode. The vicor frit can hit the bottom of the container
 4. Take the solvent/electrolyte solution and fill the electrode $\frac{1}{3}$ to $\frac{2}{3}$ of the way full
 5. Attach the septum to the top of the electrode.
 1. Using a spatula will help
 6. Put the wire/septum into solution and close the septum over the top of the glass tubing. Connect the reference electrode to part of the silver wire that is sticking out the top of the septum.

3.6. Experimentation

1. Add the redox species to the traditional electrochemical cell
2. If you're only adding one electrochemical species make sure you're scanning in the correct direction for the species that you have
3. Do not stir while collecting the CV, the solution must be quiescent